UNIVERSITY OF BIRMINGHAM

University of Birmingham
Research at Birmingham

Smart sop architectures and power control managements between light DC railway and LV distribution network

Kamel, Tamer; Tian, Zhongbei; Tricoli, Pietro

Link to publication on Research at Birmingham portal

SMART SOP ARCHITECTURES AND POWER CONTROL MANAGEMENTS BETWEEN LIGHT DC RAILWAY AND LV DISTRIBUTION NETWORK

Tamer Kamel [*1], *Zhongbei Tian* [*], *Pietro Tricoli* [*]

[*] *Department of Electronic, Electrical and Systems Engineering*
University of Birmingham, Birmingham, United Kingdom
[1] *(Corresponding author:* t.kamel@bham.ac.uk *)*

Keywords: SMART SOFT OPEN POINT, LIGHT RAILWAY NETWORK, DISTRIBUTION NETWORK, ENERGY STORAGE SYSTEM, RENEWABLE ENERGY SOURCES

Abstract

This paper presents different architectures of smart soft open points to interface electrified DC railways and low voltage power distribution networks. Both networks have similar objectives of power losses reduction, preserve network stability even with a high penetration of renewable energy sources, and accommodate new energy sectors such as electric vehicles and energy storage systems. The proposed smart soft open points will enable a flexible inter-exchange of electrical power between the two networks in order to achieve these challenging objectives. Different power management control approaches are provided in this paper according to the traffic conditions on the railway network as well as the power and voltage conditions of the distribution network.

1   Introduction

Soft open points (SOPs), also named soft normally open points, are power electronic converters used in power distribution networks to substantially improve the control of the power flow in comparison to traditional normal-open points (NOP) and normal–closed points (NCP), as Fig.1 shows. Both radial (normally open) and mesh (normally closed) distribution networks have several advantages and disadvantages. Radial networks are simple but not very reliable. Conversely, meshed networks offer a degree of redundancy to continue power supply in case of faults, but require more complex protection arrangements [1-2]. For this reason, SOPs are the best candidate to design hybrid networks, where the topology can be actually switched from radial to meshed and vice-versa depending on the actual network conditions. SOPs can control the flow of the active and reactive powers and regulate the voltages between different nodes of the distribution network. They could also be used to change the configuration of the network to supply loads isolated by faults, or provide isolation to disturbance and faults on one feeder in the network and not to mitigate the fault to other feeders. Previous technical literature has thoroughly presented different structures and control approaches of SOPs for medium voltage power distribution networks and demonstrated the improvements of network operations [3-5]. However, the application of SOP technology between railway and distribution networks has not been investigated so far. Both networks would benefit from a more integrated design, and specifically: i) reduction of power losses, ii) preservation of grid stability in scenarios with a high penetration of local renewable energy sources (RES), iii) accommodation of charging station for electric vehicles (EVs), electrical energy storages and prosumers. Additionally, electrified railway networks can enhance the stability of power distribution grids providing ancillary services and inter-exchange of electricity. However, such potential is still unexploited and it specifically addressed in this research.

This paper proposes new sSOP architectures based on power electronic converters to interface electrified dc railway network with low voltage power distribution networks. Considering the different dynamic characteristics of the two networks, the dc bus of the sSOP is used to connect an energy storage system (ESS), thus allowing a decoupling of the power flows. The new sSOPs is capable of capturing the regenerative energy of rail braking and can use it to either charge the ESS, support the LV distribution network, or both. Similarly, the excess of power generation within the LV distribution network, generated by RES but not consumed locally, can be also stored in the ESS. Therfore, the new sSOPs can react to the changes of both networks and achieve an optimised configuration without system disruptions. The paper presents a two-converters and a three-converter topology for the sSOP: to, that have been analysed through time-domain simulations for different operational states of the trains and voltage and power levels of the LV distribution network. Finally, a discussion and comparison for prospective architecture scenarios are provided with respect to controllability, power losses, braking efficiency, cost, and required spacing.

2 Light DC Railway Network

A schematic for a standard DC railway network is illustrated in Fig.2. DC railway substations are supplied from a medium voltage AC network, which is sufficiently capable to supply the railway network with three time of its nominal ratings [6] within defined period of time.
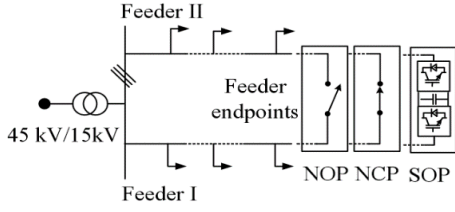
Fig.1 A simple distribution network with two feeders showing NOP, COP, and SOP interconnections

Train operations can be categorised into three main modes [7]: accelerating, coasting and braking. A fourth driving (cruising) can be included only when the distance between the two stations is relatively long. Fig.3 (a) and (b) show respectively an example of the train speed and mechanical power versus time in the three main modes in sequence.

A braking resistance (R_B) is included on board in the train to dissipate all the regenerative braking power that cannot be directly used by other trains in the network. This is because dc electrification networks are not receptive due to the diode rectifier substations and reverse braking power would cause anunacceptable increase of the dc voltage. The insertion of the braking resistance is controlled by the rail voltage (V_{Rail}); for example, for 750 V railways, the braking resistance is connected when $900 V < V_{Rail} < 1000V$.
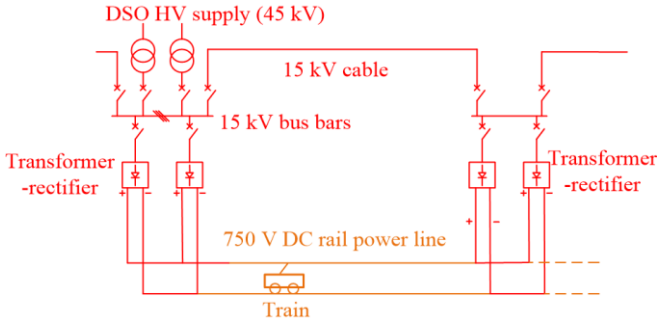

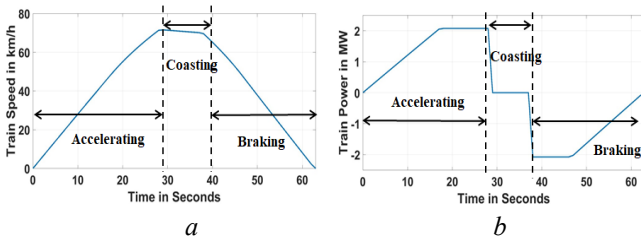Fig.2 Schematic for light DC railway networks

Fig.3 Typical operational modes of a DC train (i.e. metro)
(a) speed profile (b) power profile

A MATLAB Simulink model for the railway shown in Fig. 2 has been built as indicated in Fig.4. The railway power supply is modelled l by a constant dc voltage, $V_{Sn.L}$, representing the no load voltage of the dc supply, with in series a resistance, r_{Rec}, estimated from the voltage and current output characteristics of the rectifier bridge. The train in this model is simulated by a power controlled load current based on the provided train power given in Fig.3(b). The rail resistance,

r_{Rail}, represent the combined resistance of the electrical cable of the electrification network and return cable. Finally, the braking resistance, R_B, is connected in parallel through a switch controlled by V_{Rail}. The waveforms for the rail voltage, V_{Rail}, train current, I_{Rail}, rail supply current, I_S, and braking resistance current, I_{RB}, are illustrated in Fig.5. A chopped voltage is shown in the V_{Rail} waveform during the braking period of the train when I_{Rail} is negative, denoting a regenerative reverse current that in this example is not used by any other train.
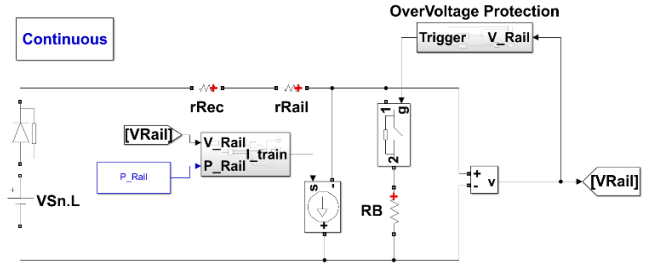

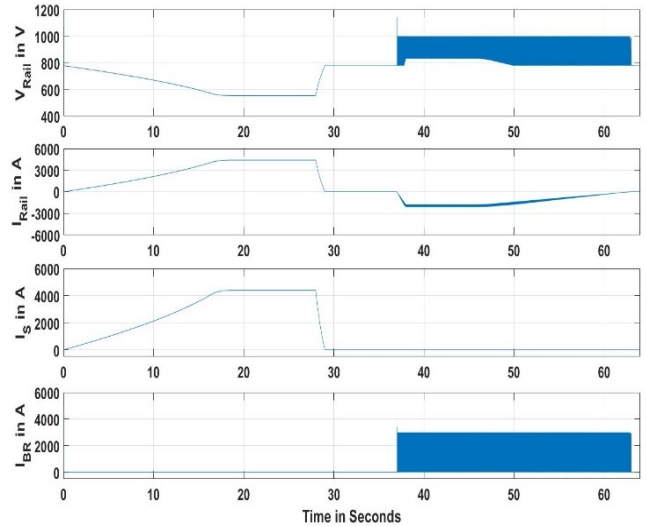Fig.4 MATLAB Simulink model for the railway network under study

Fig.5 Waveforms of V_{Rail}, I_{Rail}, I_S and I_{RB}

3 Smart SOP Between Light DC Railway Network And LV Distribution Network

The proposed sSOP structure for the interconnection between the DC railway and LV distribution network is shown in Fig.6. It has a three-terminal configuration in order to connect to the railway network, the ESS, and the distribution network. In the following the chosen ESS is a battery, because of its capability of storing an adequate level of energy to effrively decouple the operations of the two networks. The LV distribution network under considerationoperates at 400V and can act as electrical power load or power source based on the electrical loads (the industrial, residential, etc.) as well as the renewable energy sources, photovoltaic (PV) panels or wind turbines, connected to it. Several standards [8-9] have established the regulations of the connection of the disturbed generation (DG)

to the grid specially the low voltage distribution network. Moroever, The control for the power flow between the DG and public grid is manged through a number of control approaches such as drooped-control approach, along with voltage related control mode and power related control mode. Fig.7 presents the connection of the SOP to the LV public grid in which the SOP is represented as a controlled voltage source and r is the line impedance (which is mainly resistive one especially for low voltage public grids [9]). The equations for the active (P) and reactive powers (Q) between the SOP and public grid are provided as follows [9]
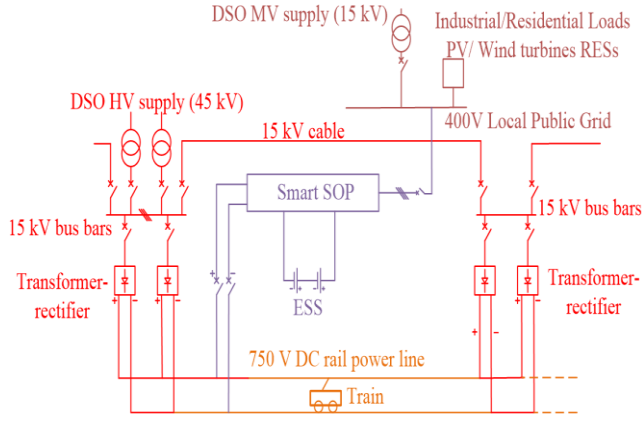

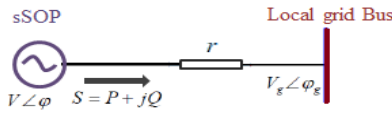Fig.6 Structure of the proposed three-terminal smart SOP

Fig.7 Equivalent circuit of SOP unit connected to the public grid bus

$$P = \frac{1}{r} \times V \times \left(V - V_g . cos(\delta)\right) \qquad (1)$$

$$Q = -\frac{1}{r} \times V \times V_g \times sin(\delta) \qquad (2)$$

$$\delta = \varphi - \varphi_g = \int\left(\omega - \omega_g\right) \times dt \qquad (3)$$

Where;

V: Voltage amplitude reference of a SOP

V_g: Voltage amplitude of the grid

r: Line impedance

δ: Power angle between the two voltages

ω: Angular frequency reference of the three-phase output of the inverter

ω_g: Angular frequency reference of the three-phase grid voltage

Two control constraints have to be defined to avoid power recirculation between the 2 networks and, hence, minimise power losses:

  i.   the dc railway substation does not feed directly neither the battery nor the public grid network.
  ii. The battery and the public grid do not supply the railway network.

These two constrains are fundamentally implemented since one of the main objectives of this smart SOP is to minimize

the mutual losses in the railway and public grid networks Accordingly, the proposed control strategies mainly investigate the benefits of the utilisation of the available power from the regenerative braking of the trains to feed the battery, the public grid, or both. The possibility of supplying the railway network from the battery or the public grid is instead less relevant, because they typically have power rating substantialy smaller to make an effective contribution. Therefore, in order to analysis the functionalities of the power electronic converters utilised in the sSOP, two different control scenarios are proposed in this paper according to whether the public gridsupplies or sinks power. This fundamentally depends on the aforementioned control algorithm for the public grid in which, if P is greater than zero, the public grid is sinks power and vice versa, according to (1).

In the 1st control scenario, as shown in Fig. 8, the public grid is a load, so it can receive any available power from the sSOP up to the grid maximum power constrain (P_{Gmax}) determined by the regulations of the provider of the public grid. If there is no available braking power from the railway network, the public grid will be fed only by the battery. On the other hand, if there is regenerative braking power from the railway network, this power is used to supply the local grid up to P_{Gmax} as well as to charge the battery with its maximum charging rate, $C_{ratemax}$. Priority will be given to feed the public grid rather than the battery to use energy directly and, hence, avoid power losses connected with the energy storage.

In the second scenario, shown in Fig. 9, the public grid supplies power to the s SOP that is representing a situation where there is extra power available from the RES. In this case study the RES is a PV energy source with variable output power during the day time. This output power will be assumed as a constant value (P_{GS}) during one mission profile of the train, which is few minutes long. Furthermore, it is assumed that the power P_{GS} can't charge the battery up to its $C_{ratemax}$. Therefore, the braking power from the railway will contribute to charging the battery up to $C_{ratemax}$ during the braking period of the train

4   Proposed Architectures Of The Smart SOP

This section studies the two– and three- converters topologies according to the proposed control strategies and scenarios.
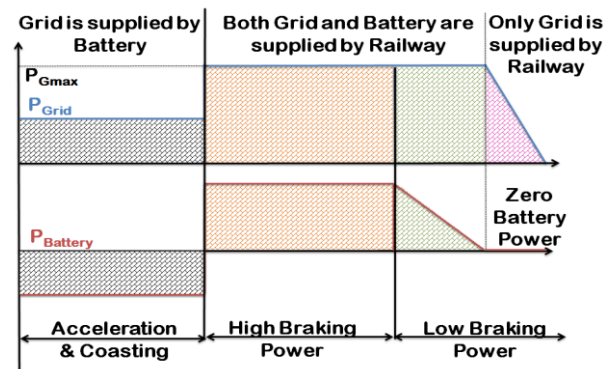

Fig.8 Proposed control power management for the 1st control scenario (grid sinks power)
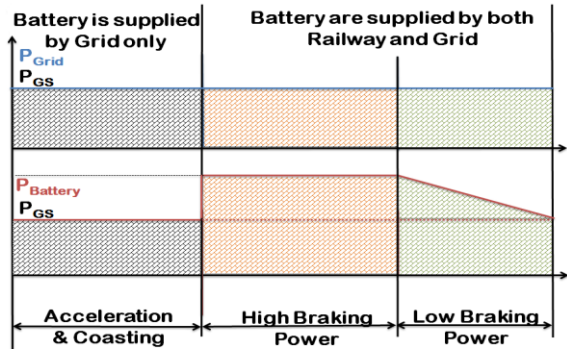
3

Fig.9 Proposed control power management for the 2nd control scenario (grid supplies power).

4.1 Two-converter topology of the smart SOP

Fig. 10 illustrates the schematic for the two-converter topology of the sSOP, in which the ESS (battery) is connected directly to the common dc bus without an additional converter. A MATLAB Simulink model for this system is demonstrated in Fig.11.

There are two controlling indicators in the MATLAB module: one for detecting the start of the train braking state, and the other to determine when the braking power is lower than the grid maximum power. The public grid and the inverter circuit of the sSOP are simulated as a power controlled current source, in which the grid power is governed by the control strategies described in the previous section.

Lithium-Ion battery cells by Panasonic , model CGR18650AF, are utilised in this study with a nominal voltage ,V_n, of 3.3 V and rated capacity,I_{Ah}, of 2 Ah [10] . According to the datasheet, the maximum charging rate $C_{ratemax}$ is 0.7 C and the maximum discharging rate is 2C. The selected battery capacity for this study has been chosen to be equal to the available braking energy of the train, which from Fig.4 is calculated as 35.57 MJ, or 9.88 kWh. In the first control scenario, when the grid acts as a load, P_{Gmax} is assumed to be 80 kW. Fig. 12 illustrates the power waveforms of the railway supply (P_S), train power (P_{rail}), battery power (P_B), and finally grid power (P_G). In the 2nd control scenario, when the grid acts as a supply, P_{GS} is assumed to be equal to 3 kW and the results are shown in Fig. 13, where the quantities are the same as those in Fig.12.
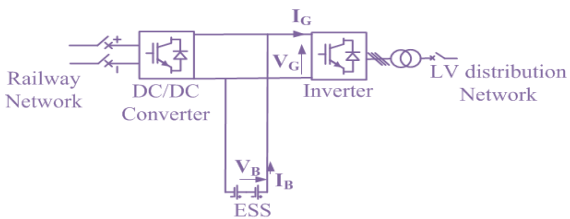

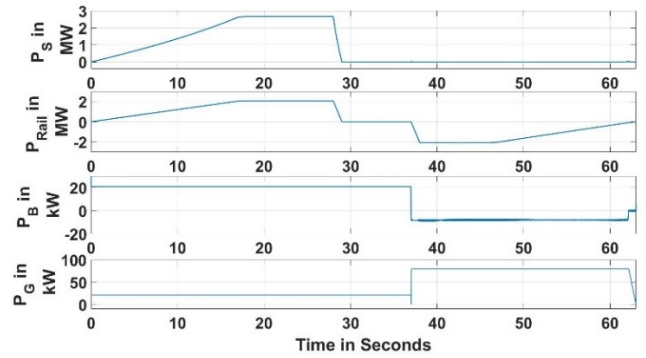Fig.10 Structure of the two-converter topology smart SOP

Fig.12 Waveforms of P_S, P_{Rail}, P_B, and P_{Grid} of the 1st control scenario for SOP two-converter topology
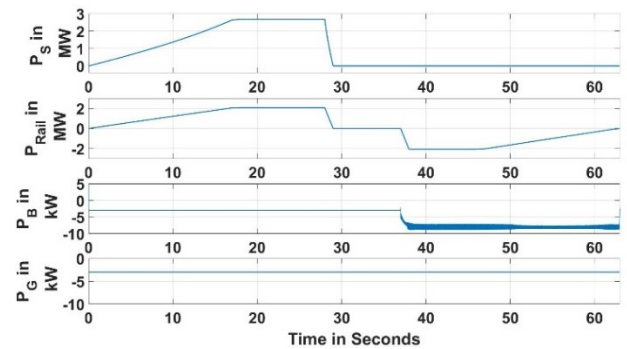

Fig.13 Waveforms of P_S, P_{Rail}, P_B, and P_{Grid} of the 2nd control scenario for SOP two-converter topology
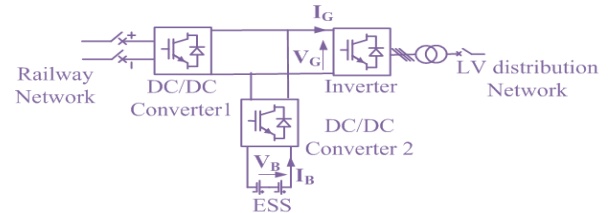

Fig.14 Structure of the two-converter topology smart SOP

4.2 Three-converter topology of the smart SOP

The schematic for the three-converter topology for the sSOP is shown in Fig.14, in which the battery is connected through another dc/dc converter. The MATLAB Simulink model for this system is given in 15. The controlling indicators, the model of the grid and the sSOP inverter and the battery are the same of the previous case. The control algorithm for the additional DC/DC converter (no.2 in the fig.14) is current based control approach dependant of the charging and discharging rate of the battery model according to its datasheet On the other hand, the DC/DC converter 1 of fig. 14 is governed by voltage based control to output fixed reference voltage of 750V for this study during all operational modes of the train.
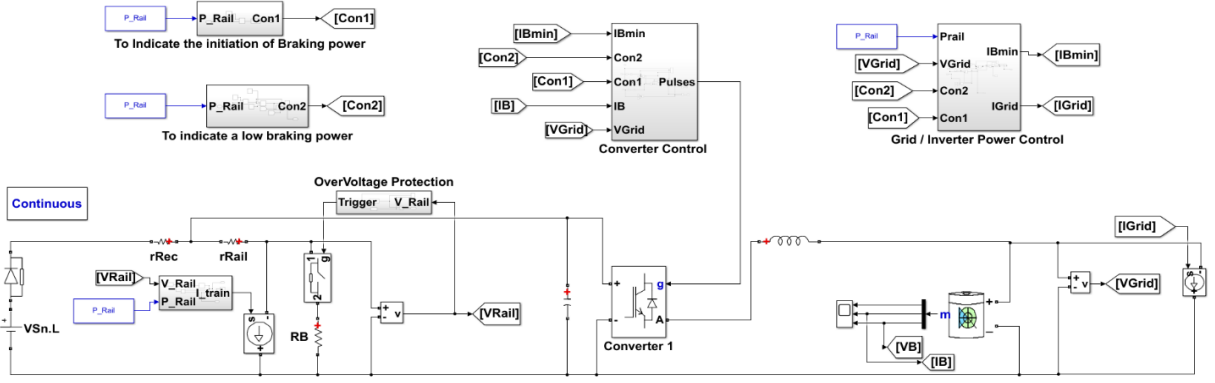
4

Fig.11 MATLAB Simulink model for the proposed two-converter topology of the smart SOP

P_{Gmax} for the 1st control scenario in this topology is assumed to be equal 80 kW similar to the other topology. P_{GS} in the 2nd control scenario of this topology is also assumed to be equal 3 kW likewise the other topology. Figures 16 and 17 illustrate the waveforms of the same parameters of figures 13 and 14 respectively but under the 2nd SOP topology of a three-converter topology.

5 Comparisons and Discussions

The energy and the power calculations of the battery and the grid during the train braking state of the railway are provided in Table 1 for both control scenarios and for both sSOP topologies. Furthermore, Furthermore, resultant storage energy and power into the battery $E_{B(st.)}$ and $P_{B(st.)}$ in these conditions are also calculated by taking into account the power losses in the internal resistance of the battery cells. Finally, the train braking efficiency for both control strategies has been calculated with this equation:

$$\eta_{Braking} = \frac{P_{B(st.)} \pm P_G}{P_{Braking}} \qquad (4)$$

Where;

$\eta_{Braking}$: Train braking efficiency
$P_{Braking}$: Train braking power
$P_{B(st.)}$: Battery storage power
P_G: Grid power; positive (grid sinks power) and negative (grid supplies power)

In accordance to the theoretical analyses and calculations, both topologies have relatively similar braking efficiency in both scenarios. However, these efficiencies don't take in account the power losses within the power converter circuits, as the three-converter topology has more power losses in comparison to the two-converter one due to the additional dc/dc converter. Furthermore, in the three-converter topology the voltage of the dc bus is very sensitive to variations of V_{Rail}, which is not mitigated by the large capacitance offered by the battery. Moreover, additional cost and space are needed for the three-converter topology. On the other hand, the drawback of the two-converter topology is the possible reduced lifetime of the battery, due to the high frequency current compomts generated by the the two converters, although this could be partially mitigated by inserting a capacitor in parallel to the battery.

For both topologies, one of the method to improve the braking efficiency is to increase the battery total capacity. In this paper, the capacity is equal to the total train braking energy, but the simulations show that it is not possible to transfer all that energy to the battery because the power is too high and exceeds $C_{ratemax}$, especially at the beginning of the braking period.

However, increasing the battery capacity will increase $C_{ratemax}$ and then enable a larger proportion of the energy recovery, although the energy transferred from the train will be less than the battery capacity. This efficiency increase must be traded off against the higher purchase cost of the battery, so it is necessary to do more in-depth investigations on the optimal efficiency level of the system.
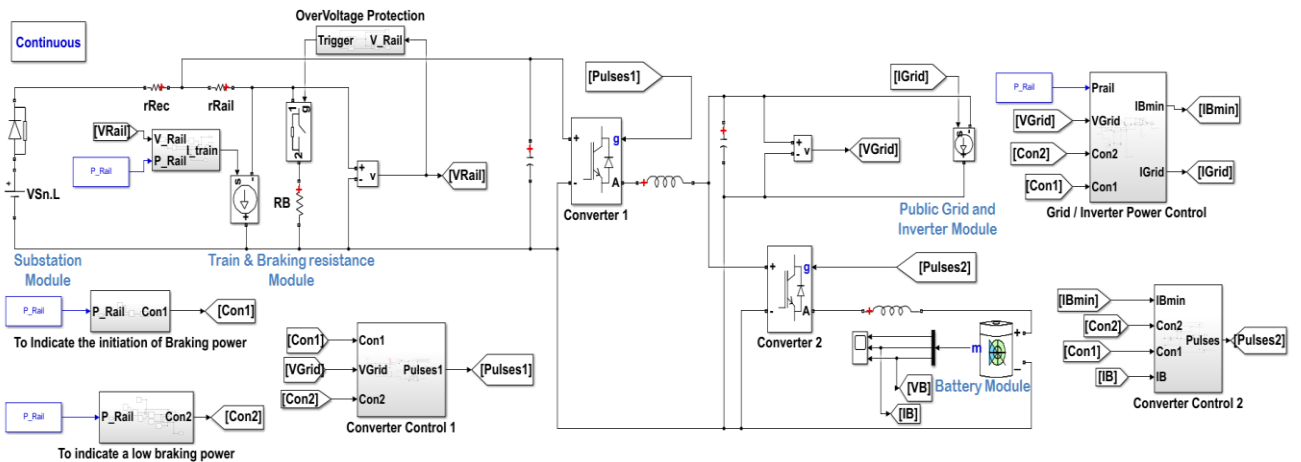

Fig.15 MATLAB Simulink model for the proposed three-converter topology of the smart SOP
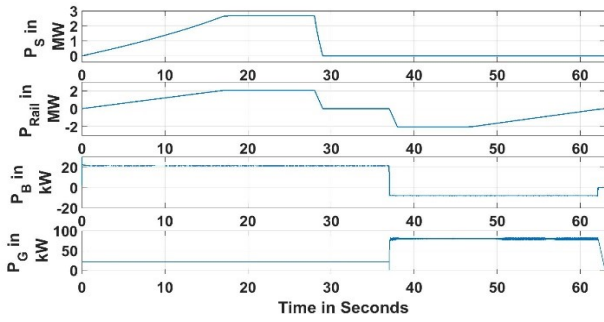
Fig.16 Waveforms of P_S, P_{Rail}, P_B, and P_{Grid} of the 1st control scenario for SOP three-converter topology
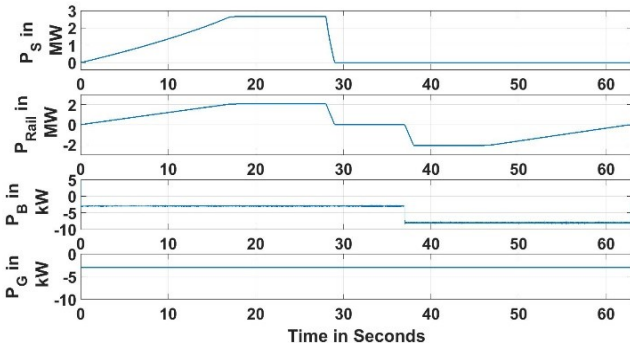

Fig.17 Waveforms of P_S, P_{Rail}, P_B, and P_{Grid} of the 2nd control scenario for SOP three-converter topology

Table 1 Energy and the power values of the battery and the grid during the train braking state

Parameter	Smart SOP two-converter topology		Smart SOP three-converter topology	
	1st Scenario	2nd Scenario	1st Scenario	2nd Scenario
$E_{G(at\ Braking)}$ (MJ)	2.04	-0.078	2.02	-0.078
$P_{G(at\ Braking)}$ (kW)	78.64	-3	77.77	-3
$E_{B(at\ Braking)}$ (MJ)	0.2	0.20	0.20	0.21
$P_{B(at\ Braking)}$ (kW)	7.81	7.99	7.756	8.05
$E_{B\_st.Braking}$ (MJ)	0.20	0.21	0.20	0.21
$P_{B\_st.(Braking)}$ kW	7.77	7.95	7.71	8.01
$\eta_{Braking}$ %	**6.316**	**0.362**	**6.248**	**0.366**

Another approach to increase the braking efficiency but with the same battery capacity is to increase $C_{ratemax}$ using different battery technologies with higher power densities. Some recent research has shown that both the charging and discharging rate of Lithium-Ion batteries can increase more than 5C [11]. Under this assumption, the braking efficiency for 5C rate would reaches 10.14% in the 1st control scenario and around 2.34% in the 2nd control scenario for both sSOP topologies. It is clear that further improvements can be obtained combining batteries with other ESS with higher power densities like supercapacitors, although the system cost and complexity would be significantly higher. It is shown that the two-converter topoplgy could be considered as more efficient and effective than the three-converter one, in which more anaylses and studies will be carried out in the future work to selet the optimal size of the ESS and converter rating along with an optimized control algorithms for the SOP operation will be implemented .

6 Conclusions

This paper proposes new smart soft open point architectures based on power electronic converters to interface electric railway networks with power distribution networks. The proposed smart soft open point provides a power connection between the two networks to achieve several objectives, including power losses reduction, preservation of network stability. Different power management control approaches of the proposed smart soft open point topologies have been analysed in this paper according to the operational states of the trains in the railway network and the grid power receptivity.

7 Acknowledgements

8 References

[1] Chen, T.H., Wei-Tzer H., Jyh-Cherng, G., et al, "Feasibility study of upgrading primary feeders from radial and open-loop to normally closed-loop arrangement", IEEE Trans Power Syst, 2004, no.19, pp1308–1316

[2] Okada, N., Kobayashi, H., Takigawa, K., et al, "Loop power flow control and voltage characteristics of distribution system for distributed generation including PV system", Proc. Photovoltaic Energy Conversion, Osaka, 2003,no.3, pp. 2284–2287

[3] Long, C., Wu, J., Thomas, L. et al, "Optimal operation of soft open points in medium voltage electrical distribution networks with distributed generation", Applied Energy, 2016, no. 184, pp.427-437

[4] Cao, W., Wu, J., Jenkins, N., et al, "Operating principle of Soft Open Points for electrical distribution network operation", Applied Energy, 2016, no.164, pp. 245-257

[5] Bloemink J., Green, T., "Increasing photovoltaic penetration with local energy storage and soft normally-open points," Proc. Power and Energy Society, USA, 2011, pp. 1-8

[6] Hill, R., "Electric railway traction, Part 3 Traction power supplies", Power Engineering Journal, 1994, pp. 275-286

[7] Tian, Z., Zhao, N., Hillmansen, S., et al, "SmartDrive: Traction Energy Optimization and Applications in Rail Systems," IEEE Trans Intell. Transp. Syst, 2019, vol. 20, no. 7, pp. 2764-2773

[8] BS EN 50438: 'Requirements for micro-generating plants to be connected in parallel with public low voltage distribution network', 2015

[9] Hou, X., Sun, Y., Yuan, W., et al, "Conventional P-ω/Q-V Droop Control in Highly Resistive Line of Low-Voltage Converter-Based AC Microgrid", Energies, 2016, vol. 9, no.11 pp.1-19

[10] Panasonic CGR18650AF Cell Specifications, 2007

[11] Kang, B. and Ceder, G., "Battery materials for ultrafast charging and discharging", Nature, 2009, 458(7235), pp.190-193.